

Monte Carlo Study of the Axial Next-Nearest-Neighbor Ising Model

Kai Zhang and Patrick Charbonneau

Department of Chemistry, Duke University, Durham, North Carolina, 27708, USA

(Dated: November 3, 2018)

The equilibrium phase behavior of microphase-forming systems is notoriously difficult to obtain because of the extended metastability of the modulated phases. We develop a simulation method based on thermodynamic integration that surmounts this problem and with which we describe the modulated regime of the canonical three-dimensional axial next-nearest-neighbor Ising model. *Equilibrium* order parameters are obtained and the critical behavior beyond the Lifshitz point is examined. The absence of widely extended bulging modulated phases illustrates the limitations of various approximation schemes used to analyze microphase-forming models.

PACS numbers: 64.60.Cn, 64.60.F-, 05.10.Ln, 75.10.-b

Microphases self-assemble in systems with competing short-range attractive and long-range repulsive interactions, irrespective of the physical and chemical nature of these interactions [1]. Microphases are the frustrated equivalent of gas-liquid coexistence for purely attracting particles. Periodic lamellae, cylinders, clusters, etc. are thus observed in a variety of systems, such as multi-block copolymers [2], oil-water surfactant mixtures [3], charged colloidal suspensions [4], and magnetic materials [5]. Although the modulated organization is spontaneous, obtaining detailed morphological control is notoriously difficult. Annealing [6], external fields [7], or complex chemical environments [8] are usually necessary to order diblock copolymers. Mesoscale periodic textures have found some technological success as thermoplastic elastomers [2] and nanostructure templates [9], but understanding how to tune and stabilize microphases is essential to broadening their material relevance.

Because experimental systems provide only limited microscopic insight into microphase formation, a number of lattice [10–13] and free-space [14–16] models have been put forward. Grasping the equilibrium properties of these models is necessary to resolve the problems surrounding the non-equilibrium assembly of microphases [17–19]. Though the modulated regime is a central feature of these systems, microphases have not been accurately characterized in any of them. Even for simple models, approximate theoretical frameworks offer only limited assistance, and treating microphases with computer simulations is so far an unresolved problem [20, 21]. In this Letter, we overcome this last issue by developing a free-energy integration method for modulated phases. We use this method to determine the phase diagram of the microphase-forming three-dimensional (3D) axial next-nearest-neighbor Ising (ANNNI) model, which has reached textbook status [21, 22], but whose characteristic modulated behavior is still not completely understood. The resulting phase information allows us to assess the validity of competing approximate treatments and to better understand the phenomenology of related experimental systems.

The ANNNI model was introduced nearly half a century ago to explain “helical” magnetic order in heavy rare-earth metals [10, 23–25]. Its Hamiltonian on a simple cubic lattice for spin variables $s_i = \pm 1$

$$H_{\text{ANNNI}} = -J \sum_{\langle i,j \rangle} s_i s_j + \kappa J \sum_{[i,j]} s_i s_j, \quad (1)$$

favors alignment of nearest-neighbor pairs $\langle i, j \rangle$, but frustrates long-range order with relative strength $\kappa > 0$ for z -axial next-nearest-neighbor pairs $[i, j]$. The coupling constant J determines the temperature T scale with Boltzmann’s constant k_B set to unity for convenience. The ANNNI model can only be solved exactly in one dimension [26], but some of its higher-dimensional features are nonetheless well understood. In 3D, the topography of the T - κ phase diagram involves three regions that join together at a multicritical Lifshitz point [27]: at high T the system is paramagnetic; at low T and κ it is ferromagnetic; at low T and for sufficiently high κ modulated layered phases form [25]. The ANNNI paramagnetic-modulated (PM) transition beyond the Lifshitz point is thought to be part of the XY universality class [28]. For $\kappa < 1/2$ the $T = 0$ ground state is ferromagnetic, and for $\kappa > 1/2$ it is the layered antiphase (“two-up-two-down”). The sequence of commensurate phases springing from the multiphase point at $T = 0$ and $\kappa = 1/2$, the structure combination branching processes at low T , and the possible occurrence of incommensurate phases are also noteworthy features of the model [29].

In order to detail the phase behavior, approximate theoretical treatments, including high- and low-temperature series expansions [30, 31], mean-field [32, 33], and other theories [34–36] have been used. Monte Carlo simulations [26, 37–39] have reliably determined the paramagnetic-ferromagnetic transition up to the Lifshitz point [40], but accurately locating transitions to and within the modulated regime has remained elusive. Even within the subset of periodic phases commensurate with the finite lattice, high free-energy barriers need to be crossed on going from one modulated phase to another. Patterns with a metastable nearby periodicity thus per-

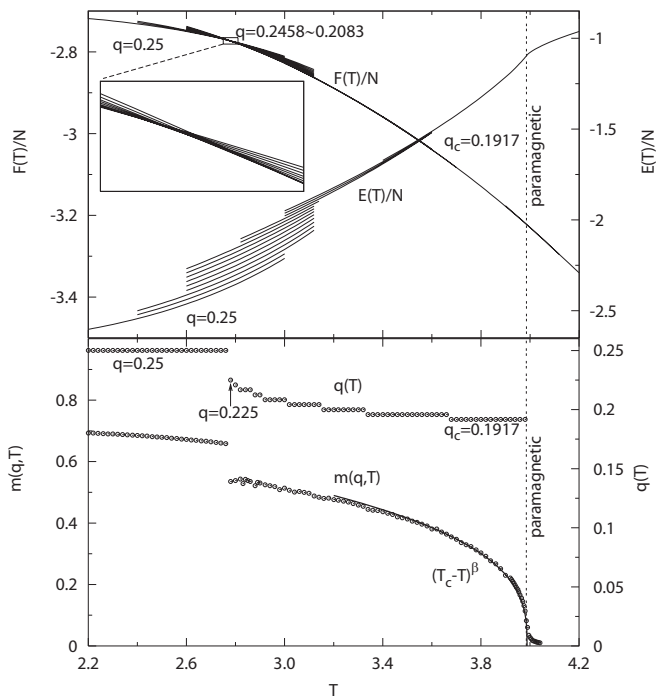


FIG. 1: (Color online) Simulation results for $\kappa = 0.7$. (Top) Energy and free energy per spin for modulations ranging from $q = 1/4$ (antiphase) to $q_c = 0.1917$ at melting. The PM transition $T_c = 3.988(1)$ (dashed line) is extracted from susceptibility measurements (Fig. 2). (Bottom) Equilibrium devil’s staircase and generalized magnetization $m(q)$. The power-law decay of $m(q)$ with $\beta = 0.34(4)$ is superimposed (line). (Inset) Snapshot of the antiphase with differently shaded beads for $s_i = \pm 1$.

sist for very long times [24, 26, 38]. Traditional simulation methodologies that facilitate ergodic sampling of phase space by passing over such barriers, notably parallel tempering and cluster moves, are of limited help in microphase-forming systems. Because the equilibrium periodicity varies with temperature, sampling higher temperatures leaves the system in a modulated phase with the wrong periodicity; because of the high free-energy barriers between modulated phases and the lack of simple structural rearrangements for sampling different modulations, the efficiency of cluster moves is limited.

We develop a simulation method based on free-energy integration to treat microphases. The free energy of modulated phases allows us to compare the stability of different periodic patterns and to reliably capture phase transitions. Some aspects of the procedure are part of the standard numerical toolkit [41], but additional specifications are in order. For a given κ , T , and wave number modulation q , we first calculate the absolute free energy F of q -modulated lamellae at a nearby reference temperature T_0 , and then thermally integrate the energy per spin E/N from T_0 to T . In the spirit of

Refs. [42, 43], the Kirkwood integration begins from decoupled spins under an oscillatory sinusoidal field with Hamiltonian $H_0 = -B_0 \sum_{i=1}^N s_i \sin(2\pi q z_i + \phi_0)$, where a small phase angle ϕ_0 is added to prevent the lattice sites from overlapping with the zeros of the field. A scaling field B_0 sufficiently strong to avoid melting is necessary for the reversibility of the integration scheme. The high free-energy barriers between the neighboring commensurate periodic patterns would also make phase transitions highly unlikely even if sections of the path are formally metastable [26]. Similarly a sinusoidal reference state is valid even if the layer profile squares at low T [26], because there is no phase transition along the integration path. We perform constant T Monte Carlo (MC) simulations on a periodic lattice with $N = L_x L_y L_z = 40^2 \times 240$, unless otherwise noted. Wave numbers $q = n/L_z$ for integer values of n keep modulations commensurate with the lattice, which leaves open the problem of incommensurate phases. Phase-space sampling gains in efficiency when single-spin flips are complemented with MC moves that take advantage of phase symmetries. In the modulated phases, layer exchanges allow for thickness fluctuations and lattice drifts sample the external field; in the paramagnetic phase, cluster moves accelerate sampling in the critical region [40]. For T_0 reference integrations, up to 10^5 MC moves (N attempted flips) are performed after 5×10^4 MC moves of preliminary equilibration.

The smooth and extended energy curves of the different modulations are characteristic of the long-lived metastable nature of the periodic phases (Fig. 1). Even over relatively long simulation times, metastable systems do not relax to their equilibrium periodicity. Thorough sampling is possible without any modulation change if the $L_x L_y$ cross-section is sufficiently large. The energy gap between neighboring phases for q ’s commensurate with the simulation box reflects the limited choice of modulations on a finite lattice. In an infinite periodic system, where all rational modulations are valid but irrational q ’s are excluded, the gap becomes infinitely small because rational numbers are dense on the real axis [38]. Although they appear to join together smoothly on the scale of Fig. 1, neighboring free-energy curves intercept. The intercept identifies the transition temperature between two modulated phases with an accuracy that vastly surpasses previous simulation approaches [37, 38]. Figure 1 illustrates the profile of the devil’s staircase for $\kappa = 0.7$ [34]. The rate of change of the equilibrium q accelerates upon cooling. The predicted discontinuity of the function before reaching the antiphase should make the staircase “harmless”, but the current numerical accuracy is insufficient to distinguish this scenario from the “devil’s last step” [10, 44].

The PM critical transition temperature T_c , which is analytically well characterized [30, 45], is used to validate the simulation results. Because the heat capacity per spin C/N is at best only weakly divergent at T_c (Fig. 2), we

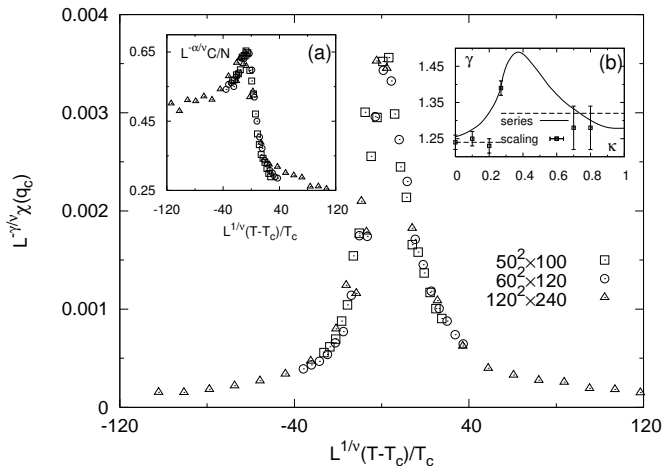


FIG. 2: Finite-size scaling of $\chi(q_c)$ at $\kappa = 0.7$ around the PM transition with $\nu = 0.60(3)$ and $\gamma/\nu = 2.13(3)$. (a) Same for C/N with $\alpha/\nu = 0.18(2)$. (b) Simulation and series expansion γ compared with Ising ($\kappa < \kappa_L$) and XY ($\kappa > \kappa_L$) exponents (dashed lines); $\kappa_L = 0.270$ result from Ref. [40]. Rushbrooke and hyperscaling equalities are obeyed within error bars.

also consider order parameters that are functions of the Fourier spin density $\tilde{s}_q \equiv \sum_{i=1}^N s_i e^{i2\pi qz_i}$ and thus naturally capture modulations. In the paramagnetic phase, the z -axis static structure factor $S(q) \equiv \langle \tilde{s}_q \tilde{s}_{-q} \rangle / N$ grows upon cooling and diverges at the critical wave number q_c obtained in Fig. 1 [26, 30]. But the system-size divergence of $S(q)$ on the modulated side makes it ill-suited for determining T_c in simulations. The generalized magnetization per spin $m(q) \equiv N^{-1} \sqrt{\langle \tilde{s}_q \rangle \langle \tilde{s}_{-q} \rangle}$ also causes problems, because it averages to zero as the lattice drifts [13]. To correct for this problem, we maximize the real component of \tilde{s}_q with a phase shift for each configuration, before taking the thermal average. The resulting function shows the characteristic power law $m(q) \sim |T - T_c|^\beta$ decay (Fig. 1). The transition is, however, most clearly identified from the generalized Binder cumulant [21] (not shown) and the generalized susceptibility

$$NT\chi(q) \equiv \langle \tilde{s}_q \tilde{s}_{-q} \rangle - \langle \tilde{s}_q \rangle \langle \tilde{s}_{-q} \rangle = NS(q) - N^2 m^2(q), \quad (2)$$

which diverges with system size $\chi(q_c) \sim |T - T_c|^{-\gamma}$ (Fig. 2) as does $\chi(0)$ at an Ising-like transition. The T_c results are in very good agreement with the series expansion [30, 45], indicating that T_c can be identified to within a part in a hundred using C from the standard lattice size. The resulting determination of the PM transition (Fig. 3) is also more reliable than the rare earlier MC results [26, 46], because of the larger system sizes used.

We also examine the suggested XY character of the PM transition [28]. The derivative of $\ln(S(q)/N)$ with J/T gives the correlation length divergence exponent ν , while the exponent ratios α/ν and γ/ν are determined by finite-size scaling of C/N and $\chi(q)$, respectively (Fig. 2) [21].

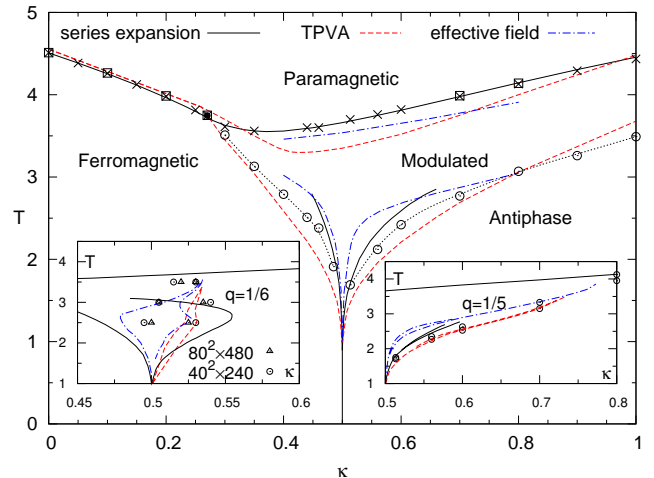


FIG. 3: (Color online) Lifshitz point (\bullet) [40] and simulation phase boundaries from $\chi(q_c)$ (\square), C (\times), and F (\odot and dotted line). High- [30, 45] and low-temperature (up to third order around the multiphase point) [31] series expansions as well as effective-field [35] and TPVA [36] results are indicated. Stability region of phases $q = 1/6$ (left inset) and $q = 1/5$ (right inset) are compared with different theoretical approaches.

The exponent ratios above κ_L , though consistent with each other, may suggest that the PM transition has a universality that is not of XY type. In particular, α has a positive sign and γ/ν is significantly different from the XY value for the ratio, which may explain the discrepancy of the series expansion γ results for large κ (see Fig. 2 and caption) [30, 45].

More significantly, the approximate treatments, which capture the external boundaries of the modulated regime reasonably well [35, 36], qualitatively disagree on the internal structure of that regime. On the one hand, as with the mean-field treatment [32, 33] and the soliton approximation [34], the effective-field method fills the modulated interior with exceptionally stable “simple periodic” [44] bulging phases, such as the “three-up-three-down” $q = 1/6$ phase and the $q = 1/5$ phase [35]. On the other hand, the tensor product variational approach (TPVA) predicts rather narrow widths for the commensurate phases [36]. The simulation results bulge less than is suggested by the first scenario. The rate of change of q with κ and T slows in certain parts of the modulated regime, but all of the phases commensurate with the periodic box are stable in turn. The stability range of the different modulated phases is overall fairly small and no exceptional stability is observed for the simple periodic phases $q = 1/6$ and $q = 1/5$ (Fig. 3), unlike for $q = 1/4$. The $q = 1/6$ phase does bulge, but increasing the system size, which allows for a more refined q selection, results in a shrinking stability range (Fig. 3), in opposition to the $q = 1/4$ phase whose stability range is system-size

independent. For the $q = 1/5$ phase, the range of stability increases slightly with κ in simulation, which is also due to the finiteness of the lattice. It is possible that the reduced range of stability of these phases compared to the mean-field predictions be related to the relatively low roughening transition ($T_r = 2.445$ [47]) in the corresponding Ising model compared to the temperatures studied here. Further study is needed to clarify this point. The absence of widely extended bulging phases suggests that the lack of qualitative agreement between observations in magnetic systems, such as CeSb [5, 48], and the mean-field stability ranges is to be expected. The commensurate phases observed are those that are kinetically accessible on experimental time scales [26] or whose stability is due to corrections beyond simple spin models. Neither effect suggests a preferable agreement with mean-field predictions.

In this Letter we have presented a methodology for simulating layered microphases, but modulated assemblies can exhibit a variety of other symmetries, under the control of an external magnetic field or by tuning the chemical potential in the corresponding lattice gas model. Generalizing the approach to other order types will greatly benefit the study of more elaborate microphase-forming systems and pave the way for studies of the non-equilibrium microphase assembly, where most of the materials challenges lie. Generalization to frustrated quantum systems is also conceivable as long as the sign problem can be surmounted [49].

We thank S. Chandrasekharan, B. Mladek, J. Oitmaa, M. Pleimling, and an anonymous referee. We acknowledge ORAU and Duke startup funding.

-
- [1] M. Seul and D. Andelman, *Science* **267**, 476 (1995).
 [2] I. W. Hamley, *The Physics of Block Copolymers* (Oxford University Press, 1998).
 [3] D. Wu, D. Chandler, and B. Smit, *J. Phys. Chem.* **96**, 4077 (1992).
 [4] A. Stradner *et al.*, *Nature* **432**, 492 (2004).
 [5] J. Rossat-Mignod, P. Burllet, H. Bartholin, O. Vogt, and R. Lagnier, *J. Phys. C* **13**, 6381 (1980).
 [6] L. M. Leung and J. T. Koberstein, *Macromolecules* **19**, 706 (1986).
 [7] K. A. Koppi, M. Tirrell, and F. S. Bates, *Phys. Rev. Lett.* **70**, 1449 (1993).
 [8] L. Meli and T. P. Lodge, *Macromolecules* **42**, 580 (2009).
 [9] T. Thurn-Albrecht *et al.*, *Science* **290**, 2126 (2000).
 [10] W. Selke, *Phys. Rep.* **170**, 213 (1988).
 [11] B. Widom, *J. Chem. Phys.* **84**, 6943 (1986).
 [12] H. Fried and K. Binder, *J. Chem. Phys.* **94**, 8349 (1991).
 [13] M. Grousson, G. Tarjus, and P. Viot, *Phys. Rev. E* **64**, 036109 (2001).
 [14] R. P. Sear and W. M. Gelbart, *J. Chem. Phys.* **110**, 4582 (1999).
 [15] J. L. Wu and J. S. Cao, *Physica A* **371**, 249 (2006).
 [16] A. J. Archer and N. B. Wilding, *Phys. Rev. E* **76**, 031501 (2007).
 [17] M. E. Cates and S. T. Milner, *Phys. Rev. Lett.* **62**, 1856 (1989).
 [18] P. Charbonneau and D. R. Reichman, *Phys. Rev. E* **75**, 050401(R) (2007).
 [19] J. C. F. Toledano, F. Sciortino, and E. Zaccarelli, *Soft Matter* **5**, 2390 (2009).
 [20] U. Micka and K. Binder, *Macro. Theo. Simu.* **4**, 419 (1995).
 [21] D. P. Landau and K. Binder, *A Guide to Monte Carlo Simulations in Statistical Physics* (Cambridge University Press, New York, 2000).
 [22] P. M. Chaikin and T. C. Lubensky, *Principles of Condensed Matter Physics* (Cambridge University Press, New York, 1995).
 [23] R. J. Elliott, *Phys. Rev.* **124**, 346 (1961).
 [24] J. Yeomans, in *Solid State Physics*, edited by E. Henry and T. David (Academic Press, London, 1988), vol. 41, pp. 151–200.
 [25] W. Selke, in *Phase Transitions and Critical Phenomena*, edited by C. Domb and J. L. Lebowitz (Academic Press, London, 1992), vol. 15, pp. 1–72.
 [26] W. Selke and M. E. Fisher, *Phys. Rev. B* **20**, 257 (1979).
 [27] R. M. Hornreich, M. Luban, and S. Shtrikman, *Phys. Rev. Lett.* **35**, 1678 (1975).
 [28] T. Garel and P. Pfeuty, *J. Phys. C* **9**, L245 (1976).
 [29] M. E. Fisher and W. Selke, *Phys. Rev. Lett.* **44**, 1502 (1980).
 [30] S. Redner and H. E. Stanley, *Phys. Rev. B* **16**, 4901 (1977).
 [31] M. E. Fisher and W. Selke, *Phi. Trans. Roy. Soc. Lond.* **302**, 1 (1981).
 [32] M. H. Jensen and P. Bak, *Phys. Rev. B* **27**, 6853 (1983).
 [33] W. Selke and P. M. Duxbury, *Z. Phys. B* **57**, 49 (1984).
 [34] P. Bak and J. von Boehm, *Phys. Rev. B* **21**, 5297 (1980).
 [35] A. Surda, *Phys. Rev. B* **69**, 134116 (2004).
 [36] A. Gendiar and T. Nishino, *Phys. Rev. B* **71**, 024404 (2005).
 [37] W. Selke and M. E. Fisher, *J. Mag. Mag. Mat.* **15-8**, 403 (1980).
 [38] E. B. Rasmussen and S. J. Knak Jensen, *Phys. Rev. B* **24**, 2744 (1981).
 [39] K. Kaski and W. Selke, *Phys. Rev. B* **31**, 3128 (1985).
 [40] M. Pleimling and M. Henkel, *Phys. Rev. Lett.* **87**, 125702 (2001).
 [41] D. Frenkel and B. Smit, *Understanding Molecular Simulation* (Academic Press, London, 2002).
 [42] B. M. Mladek, P. Charbonneau, and D. Frenkel, *Phys. Rev. Lett.* **99**, 235702 (2007).
 [43] M. Muller and K. C. Daoulas, *J. Chem. Phys.* **128**, 024903 (2008).
 [44] M. E. Fisher and A. M. Szpilka, *Phys. Rev. B* **36**, 5343 (1987).
 [45] J. Oitmaa, *J. Phys. A* **18**, 365 (1985).
 [46] F. Rotthaus and W. Selke, *J. Phys. Soc. Jpn.* **62**, 378 (1993).
 [47] K. K. Mon, D. P. Landau, and D. Stauffer, *Phys. Rev. B* **42**, 545 (1990).
 [48] Y. Muraoka, T. Kasama, T. Shimamoto, K. Okada, and T. Idogaki, *Phys. Rev. B* **66**, 064427 (2002).
 [49] M. Troyer and U.J. Wiese, *Phys. Rev. Lett.* **94**, 170201 (2005).